

Finite element analysis of stresses on adjacent teeth during the traction of palatally impacted canines

Kinan G. Zeno^a; Samah J. El-Mohtar^b; Samir Mustapha^c; Joseph G. Ghafari^d

ABSTRACT

Objective: To evaluate stresses on maxillary teeth during alignment of a palatally impacted canine (PIC) under different loading conditions with forces applied in vertical and buccal directions.

Materials and Methods: A three-dimensional finite element model of the maxilla was developed from a cone beam computed tomographic scan of a patient with a left PIC. Traction was simulated under different setups: (1) palatal spring extending from a transpalatal bar (TPB) anchored on the first molars (M1) and alternatively combined with different archwires (0.016 × 0.022-inch; 0.018 × 0.025-inch) with and without engaging second molars and (2) a buccal force against 0.018-inch, 0.016 × 0.022-inch, and 0.018 × 0.025-inch archwires with and without engaging the left lateral incisor (I2).

Results: Without fixed appliances, stresses were assumed by M1; with fixed appliances, stresses were distributed on all teeth, decreasing mesially toward the midline. Direct buccal pull exerted most stress on neighboring I2 (19–20% with different wire sizes) and first premolar (12–17%), decreasing distally, along a similar pattern with different archwire sizes. When I2 was bypassed, stresses on adjacent teeth increased only by 3–6%. Higher stresses occurred with the lighter round wire.

Conclusions: This first research on stresses on adjacent teeth during PIC traction provided needed quantitative data on the pattern of stress generation, suggesting the following clinical implications: use of distal-vertical pull from posterior anchorage (TPB) as initial movement and when using a buccal force, bypassing the lateral incisor and using heavier wires that would minimize side effects. (*Angle Orthod.* 2019;89:418–425.)

KEY WORDS: Palatally impacted canine; Finite element analysis; 3D; Biomechanics; Stress distribution; Adjacent teeth

^a Instructor, Division of Orthodontics and Dentofacial Orthopedics, American University of Beirut Medical Center, Beirut, Lebanon.

^b Graduate Student, Department of Mechanical Engineering, Maroun Semaan Faculty of Engineering and Architecture, American University of Beirut, Beirut, Lebanon.

^c Assistant Professor, Department of Mechanical Engineering, Maroun Semaan Faculty of Engineering and Architecture, American University of Beirut, Beirut, Lebanon.

^d Professor and Head, Division of Orthodontics and Dentofacial Orthopedics, American University of Beirut Medical Center, Beirut, Lebanon; and Department of Orthodontics, Adjunct Professor, University of Pennsylvania, Philadelphia, Pa.

Corresponding author: Dr Zeno, American University of Beirut, PO Box 11-0236, Medical Center, Orthodontics/Dentofacial Orthopedics, Riad El-Solh, Beirut 1107 2020, Lebanon (e-mail: kz12@aub.edu.lb)

Accepted: October 2018. Submitted: June 2018.

Published Online: December 5, 2018

© 2019 by The EH Angle Education and Research Foundation, Inc.

INTRODUCTION

The most commonly impacted tooth (1–3%)¹ after the third molars, the maxillary canine is more frequently impacted palatally. Complications during the management of the palatally impacted canine (PIC) include longer orthodontic treatment,² which was associated with the position and angulation of the tooth,^{3–5} root resorption of the adjacent teeth, particularly the lateral incisor,^{6,7} and periodontal adverse effects such as labial or palatal gingival recession.⁸ Root resorption is a progressive phenomenon that usually ceases when the canine is moved away from the incisor root.⁹

Successful PIC alignment depends on determining the direction of traction without damaging the adjacent roots. Three-dimensional (3D) imaging aids accurate localization of the canine in relation to the roots of adjacent teeth,¹⁰ helping define the correct pathway during PIC traction into the arch. Mechanical schemes advocated for PIC movement into the arch involve the

application of a “palatal-occlusal” force from the palatal side (distal-vertical)¹¹ or buccal traction.¹² Specific designs include the “ballista” buccal spring that exerts a force in vertical and transverse directions¹³ and other directional force springs.¹⁴ Several thicknesses of the supporting base archwires are advocated,^{12,13} the stiffer wires used when the traction is achieved directly to the wire with elastomeric chains.^{15,16} Mini-screws have also been used to anchor PIC traction.¹⁷

The resultant orthodontic active forces in these mechanical systems and their effects on adjacent teeth have yet to be quantified. Finite element (FE) modeling provides the optimal assessment of the physical response to a mechanical stimulus. A common noninvasive process, FE analysis allows the study of different loading conditions and consequent stresses on the teeth in a model that reconstitutes the anatomy of teeth and jaws.

While many FE studies have been reported on various orthodontic mechanics,^{18,19} FE analysis of PIC traction is limited to one publication of a single simplified model,²⁰ in which stresses on the periodontal ligament (PDL) of only the canine were evaluated in response to different force angulations. The stress distribution on the maxillary dentition, which affects the control of mechanics during PIC traction, has not been addressed previously.

The aim of this study was to evaluate the stresses on the maxillary teeth during the alignment of a PIC using different appliance designs with forces applied in vertical and buccal directions.

MATERIALS AND METHODS

This investigation was part of a broader project approved by the Institutional Review Board of the American University of Beirut (IRB ID: OTO.JG.05). The loading simulations mirrored commonly applied mechanics^{15,21,22} to sort out the effect of vertical and buccal forces on adjacent teeth. In one setup, vertical traction force was generated from a palatal spring supported by a transpalatal bar (TPB); in another setup, buccal force was applied to the canine from an archwire engaged in fixed orthodontic appliances. Variations within each situation were tested.

A cone beam computed tomography (CBCT) scan was obtained from a 16-year, 3-month-old female patient who had a maxillary left PIC. The scan consisted of 296 transverse sections with a 0.200-mm voxel resolution of the following dimensions: 400 × 400 × 296. The images were saved in DICOM format and loaded into 3D image processing software Scan IP 7.0 (*Simpleware*, Exeter, UK). The next steps included the following:

1. Model construction and meshing: The grayscale

threshold was used to segment the maxillary dentition and alveolar bone. 3D editing tools were employed to align the initially rotated premolars. The PDL was modeled by duplication and expansion of the roots of all teeth by 1.5 voxel (0.3 mm). Subsequently, the model was meshed.

2. Appliance modeling: A graphic (nonmeshed) model was imported to 3D modeling software *Solidworks Premium 2015* (Dassault Systèmes, Solidworks Corps, Providence, RI) to replicate the appliances to be tested, which consisted of (a) A TPB of 0.036-inch diameter, connected between the maxillary right and left first molars. A loop usually incorporated in the TPB was not simulated in the FE model because the appliance was passively inserted in the molars to supplement anchorage (Figure 1B–D); (b) Passive self-ligating brackets of 0.022 × 0.028-inch slot. To simplify the numerical modeling, the brackets were modeled as uniform solid attachments of dimensions 2 × 3 × 1 mm for the central incisors, right canine, and molars and 2 × 2 × 1 mm for the narrower premolars and lateral incisors. The brackets were connected through an archwire; and (c) Archwires of different cross sections: 0.018 inch, 0.016 × 0.022 inch, and 0.018 × 0.025 inch.
3. The meshed model and appliance elements were assembled in *Abaqus V6.13-1* (Dassault Systèmes).

In a first step, the model was tested for mesh convergence; the mesh converged at an element minimum edge size of 0.58 mm. The final model consisted of 639,455 tetrahedral elements and 126,476 nodes. Material properties were defined for teeth, bone, and PDL,^{20,23–25} which were assumed to be homogeneous and isotropic materials (Table 1).

The reaction stresses on the teeth were evaluated under static loading with no active sliding movement between brackets and wire. Accordingly, a tie constraint was used to model the interaction between brackets and wire, negating any relative motion between their surfaces. Also, a full constraint was used to simulate the boundary condition of the maxilla representing the attachment to the surrounding zygomatic, palatal, and sphenoid bones superiorly and posteriorly. Both constraints prevented rotational and translational motion.

A traction force of 1.0 N was applied in all investigated schemes. A total of 11 loading setups (five with vertical force, six with buccal force) were analyzed in various combinations: inclusion of TPB, changing archwire dimensions, inclusion of the second molar, and exclusion of the left lateral incisor (Figure 1). The Von Mises stress resulting from the initial force application was averaged on about 200–400 elements randomly selected around the external surface of the

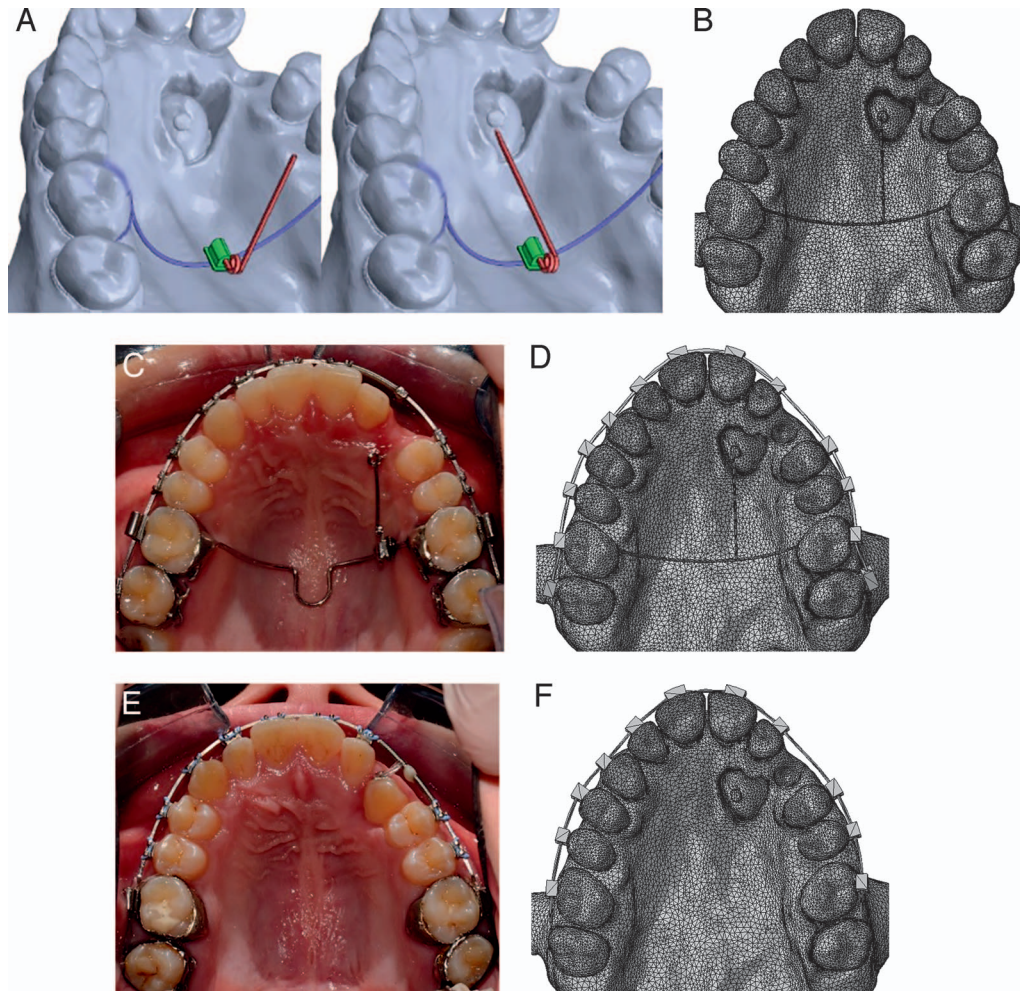


Figure 1. Meshed models of appliances tested with corresponding representative intraoral photographs. (A) Palatal spring (red) in two states: left: arm not engaged on canine; right: arm tied to canine; (B) Vertical force against a cantilever arm spring supported with transpalatal bar (TPB); (C, D) Same combination with fixed appliances engaging maxillary teeth including the second molars; and (E, F) Direct buccal force with an elastomeric chain against the base archwire.

PDL. The same element selection was used in all loading setups.

In the vertical force simulations (simulations 1–5), the force was applied upward to the free end of the spring to mimic the reaction force exerted by the PIC (ie, the resistance of the impacted canine to being pulled). To simulate the spring effect, a couple (of forces) was applied at the junction between the spring and the transpalatal bar. The moment of the couple was obtained by multiplying the force magnitude applied at the PIC by the length of the spring arm

(Figure 1A). The effects of the force were tested under the conditions of variation in archwire dimension and inclusion of second molars (Figure 1B–D).

In the buccal force simulations (simulations 6–11), the archwire alone was used. The force was applied to the canine at a point on the wire in the middle of the space reserved for the PIC alignment. The effects of three different wire dimensions and the exclusion of the left lateral incisor were tested (Figure 1D).

RESULTS

The vertical force resulted in only the molar teeth withstanding the reactive forces (3.15 and 3.31 kPa on left and right sides, respectively; Table 2; Figure 2A). Distal root tip was noted on the first molars (Figure 2B–D). When an archwire engaged the maxillary teeth, the molars withstood the bulk of the reactive force, the corresponding stresses ranging (with various arch-

Table 1. Material Properties Used in the Finite Element (FE) Model

Material	Young's Modulus, MPa	Poisson's Ratio
Stainless steel	180,000	0.3
Tooth	20,000	0.2
Bone	15,750	0.33
PDL*	0.68	0.45

* PDL indicates periodontal ligament.

Table 2. Von Mises Stress (kPa) and Corresponding Percentages (in Brackets) on Adjacent Teeth With Different Appliances Used to Move a Maxillary Left Palatally Impacted Canine Vertically (Scenario 1)^a

Setup	Wire, Inches	Von Mises Stress on PDL of Teeth, kPa													Total*
		Right							Left						
		7	6	5	4	3	2	1	1	2	4	5	6	7	
TPB cantilever															
1	None		3.31 [51.20]											3.15 [48.80]	6.46
TPB with fixed appliance															
2	0.016 × 0.022		1.55 [21.72]	0.47 [6.65]	0.41 [5.68]	0.31 [4.34]	0.30 [4.22]	0.44 [6.13]	0.29 [4.11]	0.37 [5.16]	0.61 [8.52]	0.82 [11.50]	1.57 [21.96]		7.13
3	0.016 × 0.022	0.62 [8.41]	1.46 [19.94]	0.44 [5.99]	0.39 [5.28]	0.30 [4.05]	0.20 [2.69]	0.28 [3.79]	0.19 [2.63]	0.28 [3.78]	0.50 [6.76]	0.57 [7.76]	1.46 [19.86]	0.66 [9.05]	7.34
4	0.018 × 0.025		1.04 [15.87]	0.52 [8.03]	0.48 [7.37]	0.36 [5.58]	0.23 [3.50]	0.35 [5.38]	0.28 [4.25]	0.37 [5.67]	0.47 [1.82]	0.86 [13.12]	1.57 [23.97]		6.53
5	0.018 × 0.025	0.60 [8.68]	1.09 [15.87]	0.41 [5.91]	0.45 [6.51]	0.34 [4.89]	0.20 [2.98]	0.22 [3.20]	0.17 [2.41]	0.41 [5.98]	0.40 [5.87]	0.57 [8.33]	1.33 [19.37]	0.69 [10.01]	6.86

^a PDL indicates periodontal ligament; TPB, transpalatal bar.

* Total amount of stresses under specific loading setup. Numbers in bold type indicate highest stresses under specific loading setup.

wires) between 40% and 44% (1.09–1.57 kPa) on both first molars (Table 2); the stresses gradually decreased in a mesial direction (Figure 2B,C). Stresses at the molars were nearly half of those registered when the TPB was used alone.

The stress distribution patterns on the teeth were similar regardless of wire size or second molar engagement (Table 2; Figure 2B–D). However, stresses on the first molars decreased when engaging the second molars (range: 1.1–1.46 kPa, 35–40%). When the second molars were not included, the stresses were comparatively higher on all the other teeth (eg, in setup 2: range of stresses between 0.29 and 0.82 kPa on left side); the second premolar was subjected to more stress (0.82 kPa). When engaged (setup 2), the

second molars assumed more pressure (0.66 kPa on the left side) than the other teeth (0.19–0.57 kPa).

The buccal force against archwires of different sizes resulted in the adjacent teeth bearing most of the reactive forces (Table 3; Figure 3). The highest stresses were withstood by the lateral incisor (nearly 20%, setups 6, 8, and 10: 1.13, 0.97, and 0.96 kPa, respectively, with archwire sizes 0.018, 0.016 × 0.022, and 0.018 × 0.025 inches), followed by the left central incisor (15–20%), first premolar (12–17%), and second premolar (12–16%). The Von Mises stresses decreased progressively in the distal direction from the first premolar and mesially from the lateral incisor toward the contralateral first molar.

When the lateral incisor was not engaged in the archwire, the greatest stress shifted to the left central

Table 3. Von Mises Stress (kPa) and Corresponding Percentages (in Brackets) on Adjacent Teeth With Different Appliances Used to Move a Maxillary Left Palatally Impacted Canine Buccally (Scenario 2)^a

Setup	Wire, Inches	Von Mises Stress on PDL of Teeth, kPa													Total*
		Right							Left						
		7	6	5	4	3	2	1	1	2	4	5	6	7	
Fixed appliance only															
6	0.018		0.26 [4.50]	0.21 [3.61]	0.17 [3.04]	0.25 [4.32]	0.31 [5.36]	0.58 [10.04]	0.87 [15.11]	1.13 [19.56]	0.75 [12.94]	0.76 [13.17]	0.48 [8.36]		5.76
7	0.018		0.29 [5.43]	0.23 [4.28]	0.21 [3.88]	0.28 [5.21]	0.37 [6.79]	0.74 [13.68]	1.09 [20.15]		0.84 [15.56]	0.85 [15.67]	0.51 [9.34]		5.43
8	0.016 × 0.022		0.26 [5.05]	0.20 [3.89]	0.23 [4.37]	0.24 [4.59]	0.26 [5.06]	0.50 [9.57]	0.78 [15.06]	0.97 [18.65]	0.72 [13.84]	0.64 [12.25]	0.40 [7.67]		5.20
9	0.016 × 0.022		0.28 [5.76]	0.23 [4.76]	0.23 [4.74]	0.26 [5.42]	0.32 [6.54]	0.62 [12.70]	0.93 [19.22]		0.84 [17.18]	0.72 [14.81]	0.43 [8.87]		4.86
10	0.018 × 0.025		0.30 [5.81]	0.24 [4.60]	0.22 [4.17]	0.24 [4.63]	0.27 [5.12]	0.51 [9.94]	0.74 [14.34]	0.96 [18.61]	0.63 [12.13]	0.65 [12.64]	0.42 [8.01]		5.18
11	0.018 × 0.025		0.29 [5.85]	0.25 [5.1]	0.22 [4.49]	0.30 [6.1]	0.31 [6.32]	0.62 [12.55]	1.00 [20.31]		0.76 [15.49]	0.75 [15.23]	0.42 [8.57]		4.91

^a PDL indicates periodontal ligament; TPB, transpalatal bar.

* Total amount of stresses under specific loading setup. Numbers in bold type indicate highest stresses under specific loading setup.

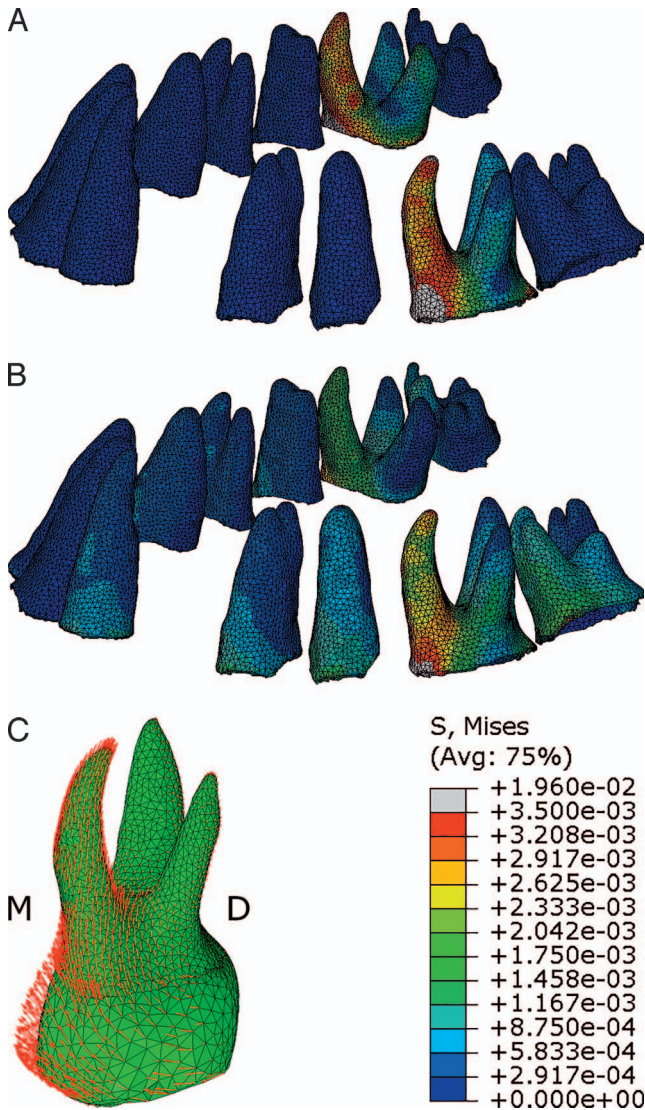


Figure 2. (A, B) Von Mises distribution (blue to gray reflects lower to higher stress) in the PDL of maxillary teeth in response to the activation of a vertical traction force on the left PIC. (A) Transpalatal bar (TPB); (B) TPB along with 0.018 × 0.025-inch archwire through the maxillary teeth including the second molars; (C) The simulated side effects generated by the load combination shown in A and B, demonstrating mesial crown tip (red) on the maxillary first molar.

incisor, with an increase of about 3–6%. (setups 7, 9, and 11: 1.09, 0.93, and 1.0 kPa, respectively, with archwire sizes 0.018, 0.016 × 0.022, and 0.018 × 0.025 inches), thereafter in decreasing order to the left first and second premolars, then to the right central incisor. Stresses on the remaining teeth were nearly half those on the adjacent teeth.

A transverse section at the level of the second premolars portrayed the areas of compression in the PDL on the buccal surface of the right premolar and the apical area and palatal surface of the left premolar (Figure 4).

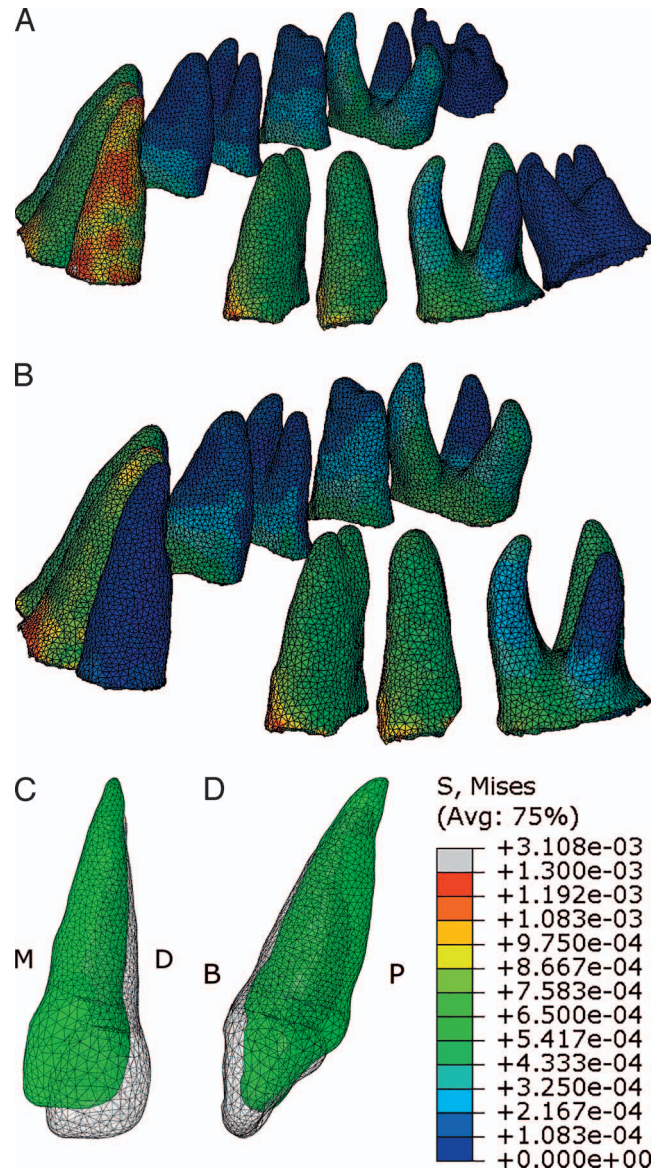


Figure 3. (A, B) Von Mises stresses in the PDL of maxillary teeth in response to the application of a buccal traction force against different archwire sizes: 0.018 inch (A); 0.018 × 0.025 inch with left lateral incisor not engaged (B). Simulated side effect (mesio-lingual tipping [C] and intrusion [D]) on the left lateral incisor (green mesh) compared to the initial position (transparent mesh) as a result of direct buccal traction against 0.018-inch archwire. The second molars were not engaged in all of these combinations.

DISCUSSION

This first research quantifying stresses generated on the adjacent teeth during PIC traction demonstrated that the use of supplementary anchorage with a vertical force consistently decreased stress on the teeth adjacent to the PIC (Table 2). When anchorage was not enhanced posteriorly, the highest stresses (30–36% of total stress) were at the adjacent first premolar and lateral incisor and/or central incisor (when the

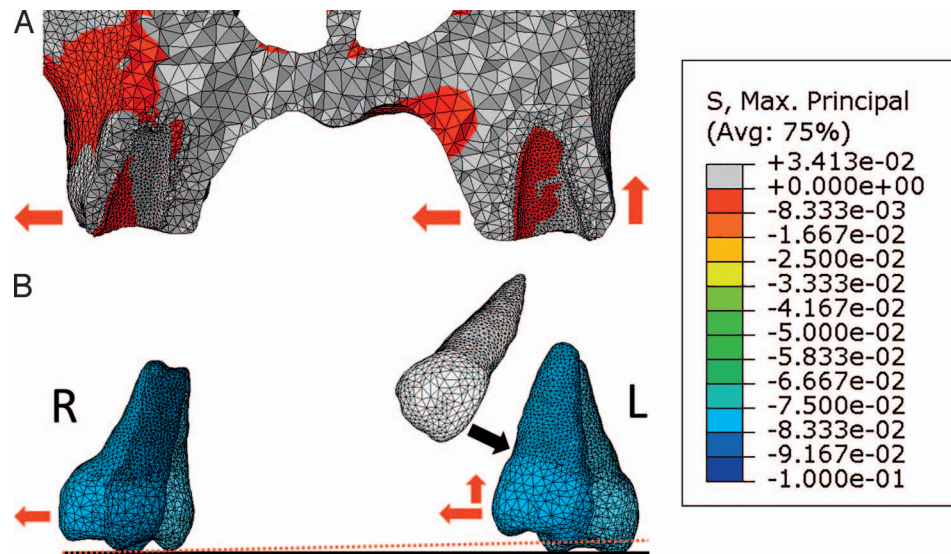


Figure 4. (A) Transverse section across the maxilla at the level of the second premolars showing maximum principal stress in the PDL of adjacent teeth (areas of compression in red). (B) Illustration of potential skewing and canting (dotted red line) of the maxillary arch (initial teeth position in transparent mesh). Red arrows (A, B) indicate the direction of reactionary forces to canine traction. Black arrow (B) represents the buccal force direction against the canine.

lateral incisor was bypassed). In the buccal setup, the first and second adjacent teeth to the impacted canine (ipsilateral premolars and incisors) endured the most stress (60–65%) (Table 3). Other than being the immediately adjacent teeth, the lateral (and central) incisors also have smaller root surface areas than do premolars and molars. These anatomical characteristics are probably related to the greater risk of root resorption, reflecting a proportionality of response in relation to tooth size.

The results suggested that to produce the least stress on the adjacent lateral incisor and premolar, distal, vertical, or a combination of both force directions would be preferable over buccal forces to steer the canine crown away from the roots of the incisors or to bring down a high PIC. Subsequently, the canine would be closer to the arch for direct buccal force activation.

Primary or supplementary posterior anchorage reduced stress on the adjacent teeth through a cantilever anchored on a transpalatal bar (or, alternatively, on a palatal temporary anchorage device). Thus, potential side effects on the anchoring molars (eg, intrusion and distal root tip) were reduced.

Stress distribution on the teeth engaged on the archwire was more uniform with increased wire dimension. Higher stresses were observed with the lighter round wire (0.018 inch) compared to the heavier archwires, which were similar in stress generation and distribution (Table 3) and subject to less deflection upon force activation. The application of a buccal force led to differential stresses between the teeth on the PIC

side, which would tip lingually, and those on the contralateral side, which would tip buccally (Figure 4). This differential movement could result in arch “skewing” that is counteracted with a full arch anchorage preparation employing rigid arch wires. Bishara¹⁵ referred to the intrusion and lingual tipping of teeth in proximity of the PIC as the “rollercoaster effect” and also advised using stiff archwires (0.018 × 0.022 inch) to offset the deflection by the PIC traction force.

Accordingly, a mechanical assembly that provides an initial activation vertically or distally through a force anchored on the molars or through a ballista-type spring would avoid the undue stresses of an initial buccal force. Subsequently, rigid archwires would avoid occlusal plane skewing.

Underlying this research was the assumption that the arch was aligned, any existing crowding resolved, and sufficient space provided for the canine before surgical exposure and traction. The basic tenet was that the reactions to initial traction on the adjacent teeth would follow the same pattern for similar force directions. Generalization of the outcomes would warrant the application of FE modeling to variable conditions, accounting for location of the canine and severity of inclination, amount of bone removal and crown clearance, and teeth and arch dimensions. Also, the remarkably time-consuming process of generating a single FE model restricted the inclusion of numerous patients. The FE model was constructed on normative assumptions that may not reflect the specific data of individual subjects and on specific experimental

settings, such as not simulating bracket slots, thus not accounting for the play between wire and bracket.

Nevertheless, the quantifiable results augment the existing literature and point to central tendencies, providing measurable proportional data that explain prior clinical observations such as the presumed higher stress on the adjacent lateral incisor.⁹ Further research would likely depict these trends with additional qualification. The variation in the transverse and sagittal position of the canine tip, rather than the canine inclination, might affect the patterns of stresses on the maxillary dentition. While this investigation focused on the initial loading of the PIC, future research should include FE modeling in parallel with clinical investigation, aiming to develop a dynamic time-dependent FE analysis to assess specific and sequential movements of the canine with differing impaction severity.

CONCLUSIONS

In this first study of stresses on adjacent teeth during initial loading on the PIC, quantified information was derived relating to force direction and appliance design.

- Direct activation with a buccal force yielded the highest stresses on the adjacent teeth, greater with round wires than with more rigid wires. Bypassing the lateral incisor eliminated the pressure on the lateral incisor and did not significantly increase stresses on the adjacent central incisor and first premolar.
- When the active appliance was anchored on the posterior molar teeth, the stress levels on the vulnerable adjacent teeth decreased. Thus, the initial vertical and/or distal force direction is critical in minimizing the effect of stress on the adjacent teeth. Supplementary anchorage through different appliances or mini-implants is recommended during PIC traction.
- Future research should include relevant impaction characteristics in order to develop more generalizable outcomes.

REFERENCES

1. Grover PS, Lorton L. The incidence of unerupted permanent teeth and related clinical cases. *Oral Surg Oral Med Oral Pathol.* 1985;59:420–425.
2. Becker A, Chaushu G, Chaushu S. Analysis of failure in the treatment of impacted maxillary canines. *Am J Orthod Dentofacial Orthop.* 2010;137:743–754.
3. Ericson S, Kurol J. Longitudinal study and analysis of clinical supervision of maxillary canine eruption. *Community Dent Oral Epidemiol.* 1986;14:172–176.
4. Stewart JA, Heo G, Glover KE, Williamson PC, Lam EWN, Major PW. Factors that relate to treatment duration for patients with palatally impacted maxillary canines. *Am J Orthod Dentofacial Orthop.* 2001;119:216–225.
5. Crescini A, Nieri M, Buti J, Baccetti T, Pini Prato GP. Orthodontic and periodontal outcomes of treated impacted maxillary canines: an appraisal of prognostic factors. *Angle Orthod.* 2007;77:571–577.
6. Walker L, Enciso R, Mah J. Three-dimensional localization of maxillary canines with cone-beam computed tomography. *Am J Orthod Dentofacial Orthop.* 2005;128:418–423.
7. Yan B, Sun Z, Fields H, Wang L. Maxillary canine impaction increases root resorption risk of adjacent teeth: a problem of physical proximity. *Am J Orthod Dentofacial Orthop.* 2012;142:750–757.
8. Szarmach IJ, Szarmach J, Waszkiel D, Paniczko A. Assessment of periodontal status following the alignment of impacted permanent maxillary canine teeth. *Adv Med Sci.* 2006;51(suppl 1):204–209.
9. Ericson S, Bjerklind K, Falahat B. Does the canine dental follicle cause resorption of permanent incisor roots? A computed tomographic study of erupting maxillary canines. *Angle Orthod.* 2002;72:95–104.
10. Chaushu S, Chaushu G, Becker A. The role of digital volume tomography in the imaging of impacted teeth. *World J Orthod.* 2004;5:120–132.
11. Becker A, Zilberman Y. The palatally impacted canine: a new approach to treatment. *Am J Orthod.* 1978;74:422–429.
12. Kornhauser S, Abed Y, Harari D, Becker A. The resolution of palatally impacted canines using palatal-occlusal force from a buccal auxiliary. *Am J Orthod Dentofacial Orthop.* 1996;110:528–534.
13. Jacoby H. The “ballista spring” system for impacted teeth. *Am J Orthod.* 1979;75:143–151.
14. Bowman SJ, Carano A. The Kilroy spring for impacted teeth. *J Clin Orthod.* 2003;37:683–688.
15. Bishara SE. Clinical management of impacted maxillary canines. In: *Seminars in Orthodontics*, Vol 4. Elsevier, Amsterdam, The Netherlands; 1998:87–98.
16. Sivakumar A, Valiathan A, Gandhi S, Mohandas AA. Idiopathic failure of eruption of multiple permanent teeth: report of 2 adults with a highlight on molecular biology. *Am J Orthod Dentofacial Orthop.* 2007;132:687–692.
17. Haydar SG, Uckan S, Sesen C. A method for eruption of impacted teeth. *J Clin Orthod.* 2003;37:430–433.
18. Holberg C, Winterhalder P, Holberg N, Wichelhaus A, Rudzki-Janson I. Indirect miniscrew anchorage: biomechanical loading of the dental anchorage during mandibular molar protraction-an FEM analysis. *J Orofac Orthop Kieferorthopädie.* 2014;75(1):16–24.
19. Suzuki A, Masuda T, Takahashi I, Deguchi T, Suzuki O, Takano-Yamamoto T. Changes in stress distribution of orthodontic miniscrews and surrounding bone evaluated by 3-dimensional finite element analysis. *Am J Orthod Dentofacial Orthop.* 2011;140:e273–e280.
20. Zhang J, Wang XX, Ma SL, Ru J, Ren XS. 3-Dimensional finite element analysis of periodontal stress distribution when impacted teeth are tracted. *Hua Xi Kou Qiang Yi Xue Za Zhi.* 2008;26:19–22.
21. Fleming PS. Multi-disciplinary management to align ectopic or impacted teeth. In: *Seminars in Orthodontics*, Vol 21. Elsevier, Amsterdam, The Netherlands; 2015:38–45.

22. Tepedino M, Chimenti C, Masedu F, Potrubacz MI. Predictable method to deliver physiologic force for extrusion of palatally impacted maxillary canines. *Am J Orthod Dentofacial Orthop.* 2018;153:195–203.
23. Bourauel C, Freudenreich D, Vollmer D, Kobe D, Drescher D, Jäger A. Simulation of orthodontic tooth movements. *J Orofac Orthop Kieferorthopädie.* 1999;60:136–151.
24. Field C, Ichim I, Swain MV, et al. Mechanical responses to orthodontic loading: a 3-dimensional finite element multi-tooth model. *Am J Orthod Dentofacial Orthop.* 2009;135:174–181.
25. Kojima Y, Fukui H. Numerical simulations of canine retraction with T-loop springs based on the updated moment-to-force ratio. *Eur J Orthod.* 2010;34:10–18.